

Temperature-dependent exciton linewidths in semiconductors

S. Rudin

*Naval Research Laboratory, Washington, D.C. 20375-5000
and U. S. Army Electronic Technology and Devices Laboratory, Fort Monmouth, New Jersey 07703**

T. L. Reinecke

Naval Research Laboratory, Washington, D.C. 20375-5000

B. Segall

Case Western Reserve University, Cleveland, Ohio 44106

(Received 13 April 1989; revised manuscript received 12 June 1990)

The temperature-dependent linewidths of excitons in semiconductors due to the interaction of the exciton with both LO phonons and with acoustic phonons are studied with use of a Green's-function approach in which the exciton-phonon interaction is treated perturbatively. The interaction between the excitons and the LO phonons is taken to be of the Fröhlich form, and the contribution to the linewidth is obtained in closed form. In this case it is found that scattering of the exciton to both bound and continuum states is important and that it is important to treat the continuum states fully as Coulomb scattering states. In describing optical-absorption processes, the fact that absorption occurs from polariton states, which are states composed of excitons coupled to light, is taken into account. The linewidths due to the exciton-LO-phonon interaction are evaluated for a series of II-VI and III-V compound semiconductors, and are shown to account for the existing experimental results for temperatures $\gtrsim 80$ K. The contributions to the linewidth due to the interaction of excitons with acoustic phonons via both the deformation potential and the piezoelectric couplings are treated, and it is found that the deformation-potential coupling dominates for all of the materials considered. Because of the small velocity of sound, scattering to only intraband intermediate states, i.e., those in which the internal exciton quantum numbers do not change, is found to contribute to the linewidth. In the case of acoustic phonons, it is found to be important to treat optical absorption as originating from polariton states in order to evaluate properly the magnitude of this contribution to the linewidth. The acoustic-phonon contribution to the linewidths is compared with experiment for temperatures $\lesssim 80$ K, for which it dominates the temperature dependence.

I. INTRODUCTION

Excitonic features dominate the emission and absorption of clean direct-band-gap semiconductors near the band gap. These features arise from phonon-assisted processes, and include the phonon-assisted exciton-absorption edge and the finite widths of exciton lines. Thus the absorption of light by the interacting exciton-phonon system is a basic problem concerning the optical properties of solids, and the temperature dependences of these features provide important information about the dynamics of this interacting system.¹⁻³

Over the years substantial experimental and theoretical work has been done to establish our understanding of the absorption process itself. Considerably less work, however, has been done to data on the related problem of the exciton linewidth due to interactions with phonons which determine the shape of the exciton-absorption and -emission lines.

Experimental studies of exciton linewidths in several II-VI materials have been made in reflectance spectroscopy,⁴ and CdS (Ref. 5) and GaAs (Ref. 6) have been stud-

ied using absorption measurements. Recently, an important development in this area has been the emergence of experimental results for exciton linewidths in semiconductor quantum wells grown by molecular-beam epitaxy, especially the GaAs/Ga_{1-x}Al_xAs system. Experimental results for exciton linewidths in these systems have recently been reported using absorption,⁷ reflection,⁸ and luminescence⁹ techniques. Excitonic features in these systems with confined geometries are of interest for possible device applications.

In this paper a formalism describing the exciton linewidths due to interactions with phonons is presented, and detailed results are given for a series of bulk systems of particular interest using the best available band masses. The interactions between the excitons and LO phonons via the Fröhlich interaction and with acoustic phonons via both the deformation-potential and piezoelectric interactions are included. A preliminary version of work along these lines was presented earlier by Segall.¹⁰ Our results for the temperature-dependent lifetimes in semiconductor quantum-well systems have been presented separately.¹¹

The basic formalism for phonon-assisted optical absorption and exciton lifetimes was developed by Toyozawa¹ and by Segall and Mahan,² and it was applied to describe absorption and emission in a number of materials by Segall.¹² These authors^{1,2} discussed light absorption by an exciton in the context of linear-response theory. The absorption then is given by the imaginary part of the exciton Green's function, and for weak exciton-phonon interaction it has a Lorentzian shape with a half-width given by the imaginary part of the exciton self-energy evaluated at the exciton resonance frequency. Apart from an asymmetry factor,² the absorption $W(\omega)$ is given by

$$\omega W(\omega) \approx \pi^{-1} |\mathcal{M}|^2 \frac{\Gamma(k, \omega)}{(\omega - \omega_0)^2 + \Gamma^2(k, \omega)}, \quad (1.1)$$

where \mathcal{M} is the optical matrix element. For energies near the exciton resonance ω_0 , the width $\Gamma(k, \omega)$ is evaluated at the exciton energy ω_0 and at exciton wave vector $k \sim 0$, which gives a Lorentzian absorption line.

Hopfield,³ however, pointed out that the interaction of light with excitons does not by itself result in light absorption, because for each wave vector \mathbf{k} and exciton internal quantum number λ the system is diagonalized by the polariton states in which energy oscillates between the photon and the exciton states. Then, true absorption requires that the polariton be coupled to a continuum of the final states such as that given by phonon scattering of the exciton.

This question was studied further by Osaka, Imai, and Takeuti,¹³ who gave a qualitative criterion for the validity of treating the exciton-photon interaction as a time-dependent perturbation. They argued that if $E_{LT}\tau/\hbar < 1$, then results like those in Eq. (1.1) based on photon-exciton perturbation theory are appropriate. Here, E_{LT} is the longitudinal-transverse exciton splitting, which measures the strength of the coupling between the photon and exciton, and τ is the polariton lifetime. On the other hand, if $E_{LT}\tau/\hbar \gg 1$, the polariton is a well-defined mode, and its damping is given in terms of Γ in Eq. (1.1), with the exciton dispersion replaced by that of the polariton.

A systematic study of the interacting photon-exciton-phonon system was given by Tait.¹⁴ He calculated the photon Green's function $D_R(k, \omega)$ in the form

$$D_R(k, \omega) = 4\pi c / [\omega^2 \epsilon(k, \omega) - c^2 k^2], \quad (1.2)$$

and obtained the dielectric function $\epsilon(k, \omega)$ by assuming a linear relation between the total vector potential in the medium and the applied current; c is the speed of light. In studying absorption, one seeks solutions at a given frequency ω , and then the absorption is given by the imaginary part of the corresponding wave vector. Solutions for the transverse modes of the system are given by the zeros of the denominator in Eq. (1.2). Here the dielectric function $\epsilon(k, \omega)$ is expressed in terms of the self-energy of the polariton rather than that of the exciton.

Tait's¹⁴ formulation provides the basis of our treatment of the line shape of the absorption near the excitonic resonance. His work justifies the criteria of Osaka *et al.*¹³

We have found that for the materials of interest in the present work, the condition $E_{LT}/\Gamma < 1$, where Γ is the total exciton linewidth, is generally satisfied. Then, the exciton line near the resonance is Lorentzian, with a half-width given by the polariton self-energy. We shall show that in the case of LO-phonon interaction, the resulting exciton linewidth is changed from that which would be obtained from a perturbation treatment of the photon-exciton interaction mainly through changes in the relevant interaction matrix elements. In the case of acoustic-phonon coupling, there are additional changes in the results arising from the difference between the polariton dispersion and that of the exciton.

In general, the temperature dependence of the width of the lowest-lying 1S exciton in semiconductors has the form¹⁰

$$\Gamma(T) = \Gamma_0 + \sigma T + \gamma N_{LO}(T). \quad (1.3)$$

The second term on the right-hand side of this equation arises from exciton interactions with acoustic phonons. The last term arises from interactions with LO phonons and is proportional to the Bose function $N_{LO}(T)$ for LO-phonon occupation. The constant term in Eq. (1.3) arises from scattering due to impurities and imperfections, and will not be considered here.

In the present work the interactions of excitons with LO phonons are described by the Fröhlich interaction. The processes involving the LO-phonon interaction are shown on the right-hand side of Fig. 1, where it is seen that the phonon can scatter the exciton to the same bound state (intraband contribution), to higher-lying bound states, and to continuum states. In the present work we obtain a closed-form expression for the contribution of the LO phonons to the linewidth by separating the Coulomb problem for the relative electron-hole motion in parabolic coordinates. We find that the contributions from both the bound and continuum states are important, and that it is important to treat the continuum states as Coulomb-scattering states rather than plane-wave states. In calculating the contribution to the exciton linewidth from acoustic phonons, both deformation-potential and piezoelectric interactions have been included. The processes involving acoustic phonons are shown on the left-hand side of Fig. 1, where it is seen that only intraband scattering contributes because of the small velocity of sound. We find that the contribution to the exciton linewidth from deformation-potential interaction is considerably greater than that from the piezoelectric interaction.

The contribution to the exciton linewidth arising from the interaction with LO phonons has been evaluated for a series of II-VI and III-V bulk semiconductors including CdS, CdSe, AgBr, ZnSe, ZnTe, GaAs, GaSb, InP, and InAs, for which experimental data are available. It is found that the continuum states contribute significantly in all cases. For example, for GaAs this contribution is about 80% of the total. The contribution to the linewidth from the interaction with acoustic phonons has also been evaluated for a series of materials of interest.

The accuracy with which the values of the effective masses are known varies from material to material. In

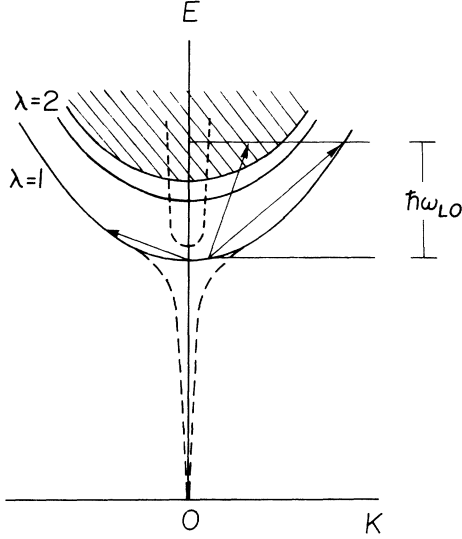


FIG. 1. Schematic illustration of the processes contributing to the phonon-induced lifetime of the lowest-lying exciton state. The solid lines indicate exciton-bound states, the hatched area indicates continuum states, and the dashed lines show the polaritons. Processes involving LO phonons are shown on the right-hand side of the figure, and processes involving acoustic phonons are shown on the left.

addition, we use the spherical approximation for the masses of the holes and electrons, thus neglecting the possible effects of nonparabolic bands and coupled valence bands. We take care to extract from the measured polaron masses the values of the bare masses to be used in the calculations. In the present work we have tested the sensitivity of the results to the imperfect knowledge of the band masses, and we find that the resulting variations in the linewidths are not especially large.

Toyozawa¹ has pointed out that if the exciton bandwidth is sufficiently small, the exciton-phonon interaction sufficiently large, or the temperature sufficiently high, the exciton line shape will be Gaussian rather than Lorentzian as a result of higher-order processes in perturbation theory. We find here that, for the materials and temperatures of interest, the conditions are such that Lorentzian line shapes result.

This paper is organized as follows. In Sec. II the basic formalism for the linewidth contributions from exciton-phonon interactions is given. In Sec. III the results for linewidths arising from LO-phonon interactions are presented. The effects on the linewidth due to coupling of the exciton and photon into a polariton are discussed in Sec. IV, and the modifications in the LO-phonon contributions to the linewidths are given. Comparison with experimental results for the linewidths due to LO-phonon interactions is also given in there. In Sec. V results for linewidths due to acoustic-phonon interactions are discussed, and the results are compared with experiment. The validity of the weak-coupling approach and of the Lorentzian line shape for the exciton absorption is commented upon in Sec. VI. Two lengthy expressions which

appear in the results for the linewidth contribution due to LO-phonon coupling are given in the Appendix.

II. EXCITON LINEWIDTHS DUE TO INTERACTIONS WITH PHONONS

The electron-hole excitations of these systems will be described in terms of excitons. The interaction of excitons with photons and phonons arises from the interactions of the electrons and holes with these excitations. It can be shown that, in a system where conduction-band electrons and valence-band holes are created and annihilated in pairs, one can rewrite the electron-phonon Hamiltonian in terms of phonon (a^\dagger, a) and exciton (B^\dagger, B) operators¹⁵

$$H_{\text{ex}} = \sum_{\lambda, \mathbf{q}} E_{\lambda \mathbf{q}} B_{\lambda \mathbf{q}}^\dagger B_{\lambda \mathbf{q}}, \quad (2.1)$$

$$H_{\text{ph}} = \sum_{\mathbf{q}} \hbar \omega_{\mathbf{q}} a_{\mathbf{q}}^\dagger a_{\mathbf{q}}, \quad (2.2)$$

$$H_{\text{ex-ph}} = \sum_{\lambda, \lambda', \mathbf{k}, \mathbf{q}} V^{\lambda \lambda'}(\mathbf{q}) B_{\lambda, \mathbf{k}+\mathbf{q}}^\dagger B_{\lambda', \mathbf{k}} (a_{\mathbf{q}} + a_{-\mathbf{q}}^\dagger). \quad (2.3)$$

At low density the excitons can be treated as bosons,¹⁶

$$[B_{\lambda \mathbf{q}}, B_{\lambda' \mathbf{q}'}^\dagger] = \delta_{\lambda, \lambda'} \delta_{\mathbf{q}, \mathbf{q}'}. \quad (2.4)$$

Here, $E_{\lambda \mathbf{q}}$ is the exciton energy for a state with internal quantum number(s) λ and center-of-mass wave vector \mathbf{q} , and $\hbar \omega(\mathbf{q})$ is the energy of a phonon of wave vector \mathbf{q} . We can write the matrix element for exciton-phonon interactions as

$$V^{\lambda \lambda'}(\mathbf{q}) = \int d^3 r \phi_\lambda^*(\mathbf{r}) \phi_{\lambda'}(\mathbf{r}) [u_{\mathbf{q}}^e \exp(-i\mathbf{q} \cdot \mathbf{r} m_e / M) - u_{\mathbf{q}}^h \exp(i\mathbf{q} \cdot \mathbf{r} m_h / M)]. \quad (2.5)$$

Here the effective-mass approximation has been used with electron and hole masses m_e and m_h . $M = m_e + m_h$ is the total mass.

For the Fröhlich interaction with LO phonons,

$$u_{\mathbf{q}}^e = u_{\mathbf{q}}^h = [2\pi e^2 \hbar \omega_{\text{LO}} (\epsilon_\infty^{-1} - \epsilon_0^{-1}) V^{-1}]^{1/2} q^{-1}, \quad (2.6)$$

where ω_{LO} is the LO-phonon frequency, V is a volume of the system, and $\epsilon_\infty, \epsilon_0$ are the high- and low-frequency values of the dielectric function.

For the deformation-potential interaction with acoustic phonons,¹⁷

$$u_{\mathbf{q}}^{e, h} = q^{1/2} (\hbar / 2\rho v V)^{1/2} D_{e, h}, \quad (2.7)$$

where v is speed of sound, D_i ($i = e, h$) are the deformation constants, and the isotropy of the elastic properties of the system has been assumed.

For the piezoelectric interaction¹⁸ with acoustic phonons,

$$u_{\mathbf{q}}^e = u_{\mathbf{q}}^h = \sum_{i, j} e q_i e_{i, j} \xi_i(\sigma, \mathbf{q}) q_j [q^2 \epsilon_0(\mathbf{q})]^{-1} [\hbar / 2\rho \omega_\sigma(\mathbf{q})]^{1/2}, \quad (2.8)$$

where $e_{i, j}$ is the piezoelectric tensor, $\xi_i(\sigma, \mathbf{q})$ is a Cartesian component of the unit polarization vector, $\omega_\sigma(\mathbf{q})$ is

the acoustic-phonon frequency, and σ indicates the three phonon polarizations.

If the exciton self-energy is evaluated to the lowest order^{1,2} in perturbation theory, these interactions contribute additively to the half-width of the Lorentzian absorption line for the lowest-lying $1S$ exciton state, which can be written

$$\Gamma_{1S} = \Gamma_{1S}^{LO} + \Gamma_{1S}^D + \Gamma_{1S}^P, \quad (2.9)$$

where, for each type of interaction,¹⁰

$$\Gamma_{1S} = \pi V \sum_{\lambda} \int d^3q (2\pi)^{-3} N(\mathbf{q}) |V_{\lambda,1S}(\mathbf{q})|^2 \times \delta(E_{1S} - E_{\lambda}(\mathbf{q}) + \hbar\omega(\mathbf{q})). \quad (2.10)$$

Here the linewidth has been evaluated at the energy E_{1S} , and

$$N(\mathbf{q}) = [\exp(\hbar\omega(\mathbf{q})/k_B T) - 1]^{-1}$$

is the Bose function for phonons.

The goal of the present work is to evaluate Eq. (2.10) for each type of interaction, taking into account all energetically available states λ .

III. LINEWIDTH CONTRIBUTION DUE TO EXCITON-LO-PHONON INTERACTION

In the effective-mass approximation the exciton energy is given by

$$E_{\lambda}(q) = E_{\lambda} + \hbar^2 q^2 / 2M, \quad (3.1)$$

where the second term represents the energy of the center-of-mass motion. By integrating over q in Eq. (2.10), we obtain, for the LO-phonon contribution to the exciton linewidth,

$$\Gamma_{1S}^{LO}(E_{1S}) = (CM/\hbar^2) \sum_{\lambda} q_{1,\lambda}^{-1} |v_{1S,\lambda}(q_{1,\lambda})|^2. \quad (3.2)$$

Here, q_1 is given by

$$\hbar^2 q_1^2 / 2M = \hbar\omega_{LO} + E_{1S} - E_{\lambda} \quad (3.3)$$

and

$$C = N_{LO}(T) e^2 \hbar\omega_{LO} (\epsilon_{\infty}^{-1} - \epsilon_0^{-1}), \quad (3.4)$$

$$v_{1S,\lambda}(\mathbf{q}) = \int d^3r \phi_{\lambda}^*(\mathbf{r}) \phi_{1S}(\mathbf{r}) [\exp(i\mathbf{q} \cdot \mathbf{r} m_h / M) - \exp(-i\mathbf{q} \cdot \mathbf{r} m_e / M)]. \quad (3.5)$$

$\phi(r)$ is an eigenfunction of the Coulomb problem given by

$$\left[-\frac{\hbar^2}{2\mu} \nabla_r^2 - \frac{e^2}{\epsilon_0 r} \right] \phi_{\lambda}(\mathbf{r}) = E_{\lambda} \phi_{\lambda}(\mathbf{r}). \quad (3.6)$$

Here, $\mu^{-1} = m_e^{-1} + m_h^{-1}$ is the optical mass of the exciton, and ϵ_0 is the static dielectric constant. The zero of energy is chosen to be at the bottom of the conduction band, so that $-E_{\lambda}$ is the exciton binding energy.

As in Eq. (1.3), we define a temperature-independent linewidth parameter γ_{1S}^{LO} ,

$$\Gamma_{1S}^{LO} = \gamma_{1S}^{LO} N_{LO}(T). \quad (3.7)$$

The matrix element $v_{1S,\lambda}$ in (3.2) for the scattering to final states in the continuum should be evaluated using the exact Coulomb wave functions. For the Fröhlich interaction, we find that it is useful to use the fact that the Schrödinger equation for the r^{-1} potential can be separated in parabolic coordinates.^{19,20} Thus we choose the functions $\phi(\mathbf{r})$ to be the eigenfunctions of L_z and A_z , where \mathbf{L} and \mathbf{A} are the angular momentum and the Pauli-Lenz operators.¹⁹ We find that the use of parabolic coordinates greatly simplifies the calculations for the contributions from the continuum part of the spectrum. Parabolic coordinates ξ , η , and α are defined by²⁰

$$x = (\xi\eta)^{1/2} \cos\alpha, \quad y = (\xi\eta)^{1/2} \sin\alpha, \quad z = \frac{1}{2}(\xi - \eta), \quad (3.8)$$

$$0 \leq \xi, \eta < \infty, \quad 0 < \alpha < 2\pi, \quad d^3r = \frac{1}{4}(\xi + \eta) d\xi d\eta d\alpha.$$

A. Discrete part of the spectrum

The bound-state energies of the exciton are given by¹⁹

$$E_n = -\frac{e^2}{\epsilon_0 a_B^*} \frac{1}{2n^2}, \quad (3.9)$$

where a_B^* is an exciton Bohr radius, $a_B^* = \hbar^2 \epsilon_0 / \mu e^2$, and n is given by

$$n = n_1 + n_2 + |m| + 1, \quad (3.10)$$

where n_1 and n_2 are non-negative integers, and m is the orbital angular momentum projection quantum number.

The exciton eigenstates are given by¹⁹

$$\phi_{n_1 n_2 m} = (\pi a_B^{*3})^{-1/2} n^{-2} f_{n_1 m}(\xi/a_B^* n) f_{n_2 m}(\eta/a_B^* n) e^{im\alpha}, \quad (3.11)$$

where

$$f_{n_1 m}(x) = \frac{1}{|m|!} \left[\frac{n_1 + |m|!}{n_1!} \right] e^{-x/2} e^{x|m|/2} {}_1F_1(-n_1, |m| + 1, x), \quad (3.12)$$

and ${}_1F_1$ is a confluent hypergeometric function.²⁰ The Q_i ($i = e, h$) are defined by

$$\mathbf{Q}_n = \mathbf{q} m_h / M, \quad \mathbf{Q}_e = -\mathbf{q} m_e / M. \quad (3.13)$$

It follows from (3.11) that $v_{1S, n_1 n_2 m} = 0$ unless $m = 0$, and so only the states with $m = 0$ contribute to (3.2).

After some lengthy manipulations, we obtain, for the contribution of the bound electron-hole states to the linewidth of the 1S exciton,

$$\gamma_{1S,dis} = \hbar\omega_{LO} \left[\frac{M}{m_0} \right]^{1/2} (R_0/|E_0|)(\epsilon_\infty^{-1} - \epsilon_0^{-1}) \sum_{n=1}^N \Delta_n(q_1) |\text{sgn}E_0 + n^{-2}B_1/|E_0||^{-1/2}, \quad (3.14)$$

where $E_0 = \hbar\omega_{LO} - B_1$, where B_1 is the binding energy of the lowest-lying exciton state [$B_1 = |E_{1S}|$ in Eq. (3.9)], $R_0 = e''m_0/2\hbar^2$. $\Delta_n(q_1)$ involves some lengthy expressions, which are given in the Appendix. The upper limit N of the summation in (3.14) depends on the material parameters and is given by

$$\begin{aligned} \hbar\omega_{LO} > B_1, \quad N = \infty \\ \hbar\omega_{LO} < B_1, \quad N = [(1 - \hbar\omega_{LO}/B_1)^{-1/2}]. \end{aligned} \quad (3.15)$$

Here, $[x]$ denotes integer part of x . For most semiconductors that we consider here, $\hbar\omega_{LO} > B_1$, and thus $N = \infty$. For large n , $\Delta_n \propto n^{-3}$, and we find that the sum

in Eq. (3.14) converges rapidly. In fact, the first few terms give most of the contribution to this sum.

B. Continuum part of the spectrum

As seen in Fig. 1, transitions to the electron-hole continuum or scattering states contribute to the linewidth if $\hbar\omega_{LO} > B_1$. This condition is satisfied for most of the materials of interest here. For the continuum states we define an energy parameter k by

$$E = \hbar^2 k^2 / 2\mu. \quad (3.16)$$

Once again, only the $m=0$ states give nonzero $v_{1S,\lambda}$. The $m=0$ eigenfunctions in parabolic coordinates are given by²⁰

$$\psi_{k\beta} = (2\pi)^{-1/2} N_{k\beta} \exp[-ik(\xi + \eta)/2] {}_1F_1(\frac{1}{2} + i\beta_1/a_B^*k, 1, ik\xi) {}_1F_1(\frac{1}{2} + i\beta_2/a_B^*k, 1, ik\eta), \quad (3.17)$$

with $\beta_1 + \beta_2 = 1$. The subscript β on ψ indicates that the function depends on one of the β_i ($i=1,2$). $N_{k\beta}$ is the normalization factor.

For these continuum states we normalize the functions on a δ function,¹⁹

$$\int dV \psi_{k\beta}^* \psi_{k'\beta'} = \delta(k - k') \delta(\beta - \beta'). \quad (3.18)$$

This requires that $\lim(\xi\psi^*\psi)_{\xi \rightarrow \infty}$ be finite. From the asymptotic behavior of the hypergeometric functions,²⁰ it follows that β_1 is real for $-\infty < \beta_1 < \infty$. In order to obtain $N_{k\beta}$, we integrate the functions in Eq. (3.17) over k and β in the form

$$\int dV \int_{k-\Delta k}^{k+\Delta k} dk' \int_{\beta-\Delta\beta}^{\beta+\Delta\beta} d\beta' \psi_{k\beta}^*(\xi, \eta) \psi_{k'\beta'}(\xi, \eta) = 1, \quad (3.19)$$

where Δk and $\Delta\beta$ are arbitrary positive intervals. We observe that as Δk and $\Delta\beta$ go to zero, the contribution from any finite volume vanishes. This allows us to use the asymptotic values of $\psi(\xi, \eta)$ for large ξ and η to evaluate Eq. (3.18). In this way we obtain the exact value of the $N_{k\beta}$,

$$N_{k\beta} = (2\pi a_B^*)^{-1} (a_B^*k)^{1/2} \exp(\pi/2ka_B^*) |\Gamma(\frac{1}{2} + i\beta_1/ka_B^*) \Gamma(\frac{1}{2} + i\beta_2/ka_B^*)|, \quad (3.20)$$

where Γ is the gamma function.

After some lengthy manipulations, we find that, for $\hbar\omega_{LO} > B_1$, the contribution of the continuum states to the linewidth parameter γ_{1S}^{LO} in Eq. (2.10) is given by

$$\gamma_{1S,cont} = 128\hbar\omega_{LO}(\epsilon_0/\epsilon_\infty - 1)(M/\mu)^{1/2} \int_0^{x_0} dx x(1+x^2)[1 - \exp(-2\pi/x)]^{-1} (F_{ee} + F_{hh} - 2F_{eh}). \quad (3.21)$$

F_{ee} , F_{hh} , and F_{eh} involve somewhat lengthy expressions, and are given in the Appendix. $x_0 = (\mu/m_0)^{-1/2} \frac{1}{2} \epsilon_0 (E_0/R_0)^{1/2}$, and the integration over x must be performed numerically. Here, m_0 is the vacuum electron mass, and R_0 is 13.6 eV.

Formulas (3.14) and (3.21) now can be used to evaluate the contributions of exciton-LO-phonon interactions to the linewidth. The parameters required for a number of materials are given in Table I. Here, m_i^* ($i=e,h$) are the

measured masses of the electron and hole, which are polaron masses. In the perturbative approach we have used here for the electron-phonon interaction, the masses that appear in the equations—strictly speaking—are bare masses that we must extract from the measurements. The polaron coupling constant for the LO-phonon interaction is^{15,21}

$$\alpha_0 = e^2(\epsilon_\infty^{-1} - \epsilon_0^{-1})(m_0/2\omega_{LO}\hbar^3)^{1/2}, \quad (3.22)$$

TABLE I. Parameters used in calculating the contribution of LO-phonon interactions to the linewidth. m_e^* , m_h^* are the experimental electron and hole (polaron) masses, $\hbar\omega_{LO}$ is the LO-phonon energy, $\epsilon_0, \epsilon_\infty$ are the experimental low- and high-frequency dielectric constants, B_1^{expt} are the experimental values of the exciton binding energies, and α_0 are the polaron coupling constants defined in Eq. (3.26). $B_1(\epsilon_0)$ is the exciton binding energy given by the simple hydrogenic formula $B_1(\epsilon_0) = \mu^* e^4 / 2\epsilon_0^2 \hbar^2$, as discussed in the text. The materials parameters and the experimental values of the exciton binding energies for all systems, except for InAs, are taken from Ref. 22. The parameters for InAs are taken from S. M. Sze [*Physics of Semiconductor Devices* (Wiley, New York, 1981)] and from D. L. Stierwalt and R. F. Polter [in *Optical Properties of III-V Compounds*, edited by R. K. Willardson and A. C. Beer (Academic, New York, 1967), Vol. 3].

	m_e^*	m_h^*	$\hbar\omega_{LO}$ (meV)	ϵ_0	ϵ_∞	$B_1(\epsilon_0)$ (meV)	B_1^{expt} (meV)	α_0
CdS	0.205	0.981	36.8	8.58	5.26	28.0	27	1.41
CdSe	0.13	0.62	26.1	9.4	6.2	12.6	15	1.25
AgBr	0.288	0.96	17.3	10.6	4.68	20	16	3.35
CdTe	0.0963	1.09	21.2	10.31	6.9	7.03	10	1.21
ZnSe	0.18	1.266	30.5	8.8	6.2	16.3	21	0.99
ZnTe	0.16	0.68	25.5	9.9	7.3	12.8	11	0.83
GaAs	0.0665	0.52	36.8	12.35	10.48	5.25	4.2	0.278
GaSb	0.047	0.32	29.8	15.7	14.4	2.02	2.8	0.118
InP	0.0803	0.58	42.8	12.6	9.6	4.7	4.0	0.442
InAs	0.023	0.4	30.5	14.6	12.3			

where m_0 is the mass of the free electron. For spherical bands in first-order perturbation theory,¹⁵ the polaron mass is given by

$$m_i^* = m_i(1 - \alpha_i/6). \quad (3.23)$$

Here the coupling constants α_i ($i=e, h$) are given by Eq. (3.22), with the electron or hole mass substituted for m_0 . For the coupled heavy- and light-hole (H, L) valence bands of zinc-blende systems, the polaron mass is given by a generalization of this form²²

$$m_{L,H}^* = m_{L,H} \left\{ 1 - \frac{\alpha_{L,H}}{6} \left[-\frac{11}{10} + \frac{3}{5} \left(\frac{m_{L,H}}{m_{H,L}} \right)^{1/2} + \frac{3}{2} \left(\frac{m_{H,L}}{m_{L,H}} \right)^{1/2} \right] \right\}^{-1}. \quad (3.24)$$

The bare electron and hole masses are obtained by inverting Eqs. (3.23) and (3.24) to lowest order in α_i .

For simplicity in the present work, we use parabolic electron and holes bands. In the case of coupled heavy- and light-hole valence bands, we use the heavy-hole mass. For ellipsoidal bands,²¹ we use the optically averaged mass, which is given by

$$m_i^{-1} = \frac{1}{3}(2m_{\perp i}^{-1} + m_{\parallel i}^{-1}). \quad (3.25)$$

These are the mass parameters given in Table I.

Results for the contributions of the exciton-LO-phonon interaction to the exciton linewidth calculated as described above for a series of materials of interest are given in Table II by the entries without asterisks. Here one sees that the relative sizes of the contributions to γ_{LO} —from intraband transitions $\gamma_{1S,1S}^{LO}$, from transitions to all of the bound states $\gamma_{1S,\text{dis}}$, and from transitions to

the continuum states $\gamma_{1S,\text{cont}}$ —vary from material to material. In general, the contribution from the continuum states is substantial; in the case of GaAs it is approximately 80% of the total. Thus it is necessary to treat this contribution accurately. In the case of exciton linewidths in semiconductor quantum wells, we have compared calculations done by us,¹¹ using the full scattering states for the continuum, with calculations done by others,⁹ in which plane-wave states were used to represent the continuum. Such a comparison suggests that the plane-wave

TABLE II. $\gamma_{1S,1S}^{LO}$ is the intraband contribution to γ_{1S}^{LO} , the parameter defined in Eq. (3.7) characterizing the total linewidth due to exciton-LO-phonon interactions. $\gamma_{1S,\text{dis}}$ is the contribution of all discrete states, and is given by Eq. (3.14) in the text. $\gamma_{1S,\text{cont}}$ is the contribution from the continuum states, and is given by Eq. (3.21).

	$\gamma_{1S,1S}^{LO}$	$\gamma_{1S,\text{dis}}^{LO}$	$\gamma_{1S,\text{cont}}^{LO}$	γ_{1S}^{LO}
CdS	24.1	34.8	27.1	61.9
CdS*	28.9	43.7	19.8	63.6
CdSe	12.9	16.5	11.7	18.3
CdSe*	15.2	18.9	10.9	29.9
AgBr	6.84	26.42	5.86	32.3
AgBr*	15.3	15.3	0	15.3
CdTe	17.8	19.6	4.82	24.5
CdTe*	22.5	24.0	2.29	26.3
ZnSe	20.0	26.1	8.48	34.7
ZnSe*	24.2	33.0	5.77	38.8
ZnTe	8.58	11.6	10.7	22.5
ZnTe*	9.32	12.8	10.3	23.2
GaAs	3.30	4.44	16.9	21.4
GaAs*	3.44	4.61	16.3	21.0
InP	6.74	9.06	33.8	42.8
InP*	6.29	8.54	35.9	44.5
InAs	1.79	2.44	9.15	11.6
GaSb	0.454	0.645	8.88	9.5

approximation for the continuum states may lead to differences in the linewidth by a factor on the order of 2.

A comparison of the results obtained above with experimental data is made at the end of the next section.

IV. POLARION EFFECT ON THE LINEWIDTH

In the preceding section we developed a formalism for calculating, perturbatively, the exciton linewidth due to the exciton-phonon interaction. We indicated in the Introduction that the resonant interaction between photons and excitons, which gives rise to polaritons, modifies the magnitude of the linewidth. Strictly speaking, in this case one is calculating the linewidth of the exciton polariton rather than that of the exciton. Various aspects of excitonic polaritons and their coupling to phonons have been discussed in the literature.^{23,14,24,25} Here we briefly discuss the effect on the linewidth of this resonant interaction between light and excitons.

The exciton-photon Hamiltonian is diagonalized by a unitary transformation^{3,25} that gives the exciton operator B as a linear combination of the polariton operators $\hat{\phi}_{ik}, \hat{\phi}_{ik}^\dagger$, where $i=1,2$, labels the lower and upper polariton branches, respectively:

$$B_{\mathbf{k}} = u_1(\mathbf{k})\hat{\phi}_{1,\mathbf{k}} + u_2(\mathbf{k})\hat{\phi}_{2,\mathbf{k}} + v_1^*(-\mathbf{k})\hat{\phi}_{1,-\mathbf{k}} + v_2^*(-\mathbf{k})\hat{\phi}_{2,-\mathbf{k}}. \quad (4.1)$$

If $E_1(\mathbf{k})$ and $W_1(\mathbf{k})$ are the lowest-lying exciton and polariton energies, respectively, measured from the top of the valence band, then in the neighborhood of the exciton-photon crossover,

$$|W(\mathbf{k}) - E(\mathbf{k})| / [W(\mathbf{k}) + E(\mathbf{k})] \ll 1, \quad (4.2)$$

and²⁵

$$v_i(\mathbf{k}) \ll u_i(\mathbf{k}). \quad (4.3)$$

Then, for ω near W_1/\hbar , we can show that¹⁰

$$|u_1(\mathbf{k})|^2 \approx \frac{E_1^2 \pi \beta_1 / \epsilon_0}{E_1^2 \pi \beta_1 / \epsilon_0 + (E_1 - W_1)^2}, \quad (4.4)$$

where β_1 is the contribution to the polarizability from the $1S$ state.

From Eqs. (2.3), (4.1), and (4.3), an approximate Hamiltonian can be written that describes the interaction of the lower-branch polaritons with phonons for energies given in (4.2):

$$H_{\text{pol-ph}} = \sum_{\lambda, \lambda', \mathbf{k}, \mathbf{q}} V_{\lambda\lambda'}(\mathbf{q}) u_1^{\lambda'}(\mathbf{k} + \mathbf{q}) u_1^{\lambda} \hat{\phi}_{1,\mathbf{k}+\mathbf{q}}^{\lambda'} \hat{\phi}_{1\mathbf{k}}^{\lambda} (a_{\mathbf{q}} + a_{-\mathbf{q}}^\dagger). \quad (4.5)$$

Then, applying perturbation theory to the polariton-phonon interaction, we obtain, for the polariton lifetime,

$$\Gamma_{1S}^{\text{pol}}(\mathbf{k}, E_{1S}) \approx \pi V |u_1^{1S}(\mathbf{k})|^2 \sum_{\lambda} \int d^3q (2\pi)^{-3} N_{\mathbf{q}} |V_{\lambda,1S}(\mathbf{q})|^2 |u_1^{\lambda}(\mathbf{k} + \mathbf{q})|^2 \delta(E_{1S} - W_1^{\lambda}(\mathbf{q}) + \hbar\omega_{\text{LO}}). \quad (4.6)$$

Here the polariton energy $W(\mathbf{k})$ is determined by²³

$$\hbar^2 c^2 k^2 / W^2 = \epsilon_0 + 4\pi\beta_1 / (1 - W^2/E^2), \quad (4.7)$$

where $E(\mathbf{k})$ is a transverse exciton energy that is given in Eq. (3.1). The result for the polariton lifetime in Eq. (4.6) replaces that for the exciton lifetime in Eq. (2.10), where $W(\mathbf{k})$ is a polariton energy, and $E(\mathbf{k})$ is a (transverse) exciton energy given by Eq. (3.1).

The linewidth is modified in two ways by the interaction that gives rise to the polariton: (i) the matrix elements in Eq. (2.10) are modified by the factors of u in Eq. (4.5), and (ii) the density of final states is changed by the replacement of the exciton dispersion $E(\mathbf{q})$ in Eq. (2.10) with the polariton dispersion $W(\mathbf{q})$ in Eq. (4.7). We find that the first effect plays a role in the case of LO-phonon coupling, and the second in the case of acoustic-phonon interactions. These modifications in the exciton linewidth are sometimes referred to as "polariton effects."

We now discuss the case of the exciton-LO-phonon interaction. The solutions at a fixed frequency, which are sometimes called "forced harmonic" solutions,¹⁴ are required in treating absorption. These solutions are given by setting the denominator of Eq. (1.2) equal to zero and

solving for \mathbf{k} at a fixed $\omega = W/\hbar$. These solutions will be near the resonance, which is given by $W_1 = E_1(\mathbf{k}=0)$, where E is measured from the top of the valence band. On the other hand, there are also solutions at a specified \mathbf{k} , which are sometimes called "quasiparticle" solutions.¹⁴ The resonance for these solutions is at the wave vector k_r , at which the exciton and photon energies crossover, and is given by

$$\hbar c k_r / \sqrt{\epsilon_0} = E_1(k_r). \quad (4.8)$$

For k near k_r , we obtain, from (4.7),

$$W \approx [E^2 + EE_{\text{LT}} - (E^2 E_{\text{LT}}^2 + 2E^3 E_{\text{LT}})^{1/2}]^{1/2}. \quad (4.9)$$

In general, $E \gg E_{\text{LT}}$, the longitudinal-transverse exciton splitting (see Table III), and then (4.9) reduces to

$$|W - E| \approx (EE_{\text{LT}}/2)^{1/2}. \quad (4.10)$$

We now consider the effects of the factor $u(\mathbf{k})$. This factor is given by Eq. (4.4), and β_1 is related to E_{LT} by the expression²³ $2\pi\beta_1/\epsilon_0 = E_{\text{LT}}/E_1$. When $|W - E| \sim O(E_{\text{LT}})$, $u \approx 1$. On the other hand, when k is close to k_r , $W \sim O(0.5(E_{\text{LT}}E))^{1/2}$, and $u \approx 0.5$. In Eq. (4.6) the factor $u_1^{1S}(k) \approx 1$ because k is determined by

TABLE III. E_1 is the exciton energy measured from the top of the valence band, and E_{LT} is the longitudinal-transverse exciton splitting. γ_{1S}^{LO} is the total linewidth parameter from LO-phonon interactions defined in Eq. (3.7). γ_{1S}^{pol} is the value of the linewidth parameter including the effects of the resonant interaction between light and excitons to form polaritons as described in the text. γ_{1S}^{expt} are the experimental values of the linewidth parameters. The values of the parameters E_1 and E_{LT} are taken from Ref. 23.

	E_1 (meV)	E_{LT} (meV)	γ_{1S}^{LO} (meV)	γ_{1S}^{pol} (meV)	γ_{1S}^{expt} (meV)
CdS	2553	1.9	61.9	59.6	41 ^a
CdTe	1595	0.4	24.5	19.8	17±7 ^b
ZnSe	2802	1.45	34.7	29.2	30±7 ^b
ZeTe	2380	0.8	22.5	19.9	16±7 ^b
GaAs	1515	0.08	21.4	17.7	7 ^c
InP	1418	0.14	42.8	35.9	

^aReference 5.

^bReference 4.

^cReference 6.

$k = k(E_1/\hbar)$. The factor in Eq. (4.5) involving $u(\mathbf{k} + \mathbf{q})$, however, is more complicated. If $q \approx k$, then, for those directions in \mathbf{q} space where $|\mathbf{k} + \mathbf{q}| < k_r$, $u(\mathbf{k} + \mathbf{q})$ can be significantly less than 1. In general, \mathbf{q} depends on λ through the δ function in Eq. (4.6), and the angular integration goes over all directions. Thus, in principle, one should perform this angular integration first and then do the sum over λ .

In the present work we use a simple approximation for the factor involving $u(\mathbf{k} + \mathbf{q})$ in Eq. (4.5). We exclude from the integral for the continuum states, which occurs in the generalization of Eq. (3.21), an interval where the integrand is significantly reduced by the angular integration. The criterion for this choice is somewhat arbitrary and is given by excluding the region $a_B^* q < (a_B^* k_r + a_B^* k_1)$, where k_r is given by (4.8), which gives

$$a_B^* k_r = (e^2/\hbar c) E_1 / 2\sqrt{\epsilon_0} B_1, \quad (4.11)$$

and k_1 is given by the polariton dispersion relation $k_1 = k_1(E_1/\hbar)$. We restrict the integration for the contribution of the continuum states to $x < [x_0 - (\mu/M)(a_B^* q_1)]$, where $q_1 = k_r + k_1$, and x_0 is defined in Eq. (A32) in the Appendix.

Discussion

Values of the longitudinal-transverse exciton splitting are given in the second column of Table III for a number of materials of interest. Results for the exciton-polariton linewidths obtained from Eq. (4.6) using the treatment of the polariton factors above are given by $\gamma_{1S}^{(pol)}$ in Table III. For comparison, the γ_{1S}^{LO} are the exciton linewidths from Eq. (2.10) without the polariton corrections (as given in the last column of Table II). The polariton corrections result in modest decreases in the magnitudes of the linewidths. For most of these materials, the polariton correction makes only modest changes in the linewidths, and thus, for them, a better estimate of the angular integration in Eq. (4.6) is not necessary. In the cases of GaAs and InP, the corrections are larger, and

better estimates of the angular integration might be useful.

The available experimental results for the LO-phonon contribution to the linewidth are given by γ_{1S}^{expt} in Table III. These results were obtained by fitting the data to a form such as that in Eq. (1.3). Experimental uncertainties are fairly large and are listed for CdTe, ZnSe, and ZnTe. In these cases the theoretical results are in agreement with experiment within the experimental uncertainties. No experimental uncertainty is given for CdS. The poorest agreement with experiment is for GaAs, which we will discuss below. It should be noted that in all cases the modifications introduced by the polariton factors reduce the calculated linewidths and bring them into better agreement with the experimental results.

We now discuss some factor involved in comparing the present theoretical results with experiment. Our treatment has been carried out systematically in perturbation theory in the exciton-phonon interaction. Thus it is proper to use the bare masses in the lifetime calculation, as discussed above. This is appropriate for systems in which the phonon energy $\hbar\omega_{LO}$ is smaller than the exciton binding energy. If $\hbar\omega_{LO}$ is larger than the exciton binding energy, there may be higher-order corrections to the exciton lifetime due to polaron self-energy effects. As seen in Table I, $\hbar\omega_{LO}$ is often comparable to the exciton binding energy. In order to estimate the upper bound to the magnitude of such higher-order effects, we have also calculated the linewidths using the polaron masses, which are indicated by asterisks appended to the material's designation in Table I. The differences between the calculations using bare masses and polaron masses vary from a few percent in a case like GaAs, for which the coupling constant α_0 is small, to a factor of 2 in the unusual case of AgBr, for which α_0 is very large.

In the present treatment the exciton mass and dielectric constants enter as parameters, and the exciton binding energy is given implicitly in terms of these parameters by the simple hydrogenic formula $B_1 = \mu e^4 / 2\epsilon_0^2 \hbar^2 = (\mu/m_0) R_0 / \epsilon_0^2$, where $R_0 = 13.6$ eV, and $\mu^{-1} = m_e^{-1} + m_h^{-1}$. Because the exciton mass and binding energy enter the theory in this way, it is not consistent to

use experimental values for the exciton binding energies, but, instead, the binding energies given by the hydrogenic formula should be used. In Table I we compare theoretical results for the exciton binding energy, denoted $B_1(\epsilon_0)$, with experimental values. Here we have used the polaron masses in the evaluation of $B_1(\epsilon_0)$. The experimental and theoretical values of the binding energy are in reasonably good agreement. The differences between the two arise from effects like central-cell corrections, which are outside of the scope of the present work.

For simplicity in the present work we have used a single parabolic band for each the electrons and the holes. For cases like GaAs, which have coupled heavy- and light-hole bands at the zone center, it is not possible to choose a single hole mass to represent properly both the center-of-mass motion of the exciton and the relative motion, which enters the exciton binding energy. The dynamic processes studied here involve scattering of the center of mass of the exciton by LO phonons. Kane²⁶ has shown that for the coupled hole bands in GaAs, for the energies of interest here, the appropriate mass for the lowest-lying exciton band is that for the heavy hole, which we have used here. As seen in Table I, the heavy-hole mass ($0.52m_0$) gives an exciton binding energy somewhat larger than that seen experimentally. The “optical mass” of the hole band, $(\mu_{hh}^{-1} + \mu_{lh}^{-1})^{-1}$, gives an exciton binding energy in better agreement with experiment. We have checked the sensitivity of our results for the linewidth to our choice for the hole mass for GaAs, and we find for GaAs that by decreasing the hole mass by a factor of 2 the linewidth is increased by 50%. We feel that in the case of GaAs a better treatment of the coupled valence band is probably necessary to obtain a quantitative understanding of LO-phonon contributions to the linewidth.

V. LINEWIDTH CONTRIBUTION DUE TO EXCITON-ACOUSTIC-PHONON INTERACTION

In the beginning of this section we will consider the propagating modes to be excitons, and calculate the linewidths due to deformation potential¹⁷ and piezoelectric¹⁸ interactions. The linewidth due to exciton-acoustic-phonon interactions will be written in terms of these two contributions as $\Gamma^{\text{ac}} = \Gamma^{\text{def}} + \Gamma^{\text{piez}}$. Later in the section we will consider the modifications in these results

arising from the fact that the initial state is a polariton. For the 1S ground state of the exciton with momentum $\mathbf{k} \approx \mathbf{0}$, energy conservation for one-phonon absorption gives

$$E_\lambda + \frac{\hbar^2 q^2}{2M} - E_{1S} - \hbar v q = 0, \quad (5.1)$$

where v is the angularly averaged sound velocity. Real solutions to Eq. (5.1) require $E_\lambda - E_{1S} < Mv^2/2$. For typical values of the parameters for materials of interest (see Table IV), this condition is satisfied only for $\lambda = 1S$, i.e., for intraband contributions, as indicated in Fig. 1. In addition, for $T \gtrsim 10$ K the Bose factor for the acoustic phonons can be expanded to give $N_q \simeq k_B T / \hbar v q$.

We first consider the deformation-potential interaction with longitudinal-acoustic phonons. Substitution of Eqs. (2.7) and (5.1) into Eq. (2.10) for $\lambda = 1S$ gives

$$\begin{aligned} \Gamma^{\text{def}}/k_B T &= (M^2/\pi v \hbar^3 \rho) \\ &\times [D_e(1 + a_B^{*2} P_e^2)^{-2} - D_v(1 + a_B^{*2} P_h^2)^{-2}]^2, \end{aligned} \quad (5.2)$$

where $P_i = m_i v / \hbar$, ρ is the density, and a is the exciton Bohr radius. Typically, $P_i a \ll 1$, and thus Eq. (5.2) becomes

$$\Gamma^{\text{def}}/k_B T \simeq (M^2/\pi v \hbar^3 \rho)(D_e - D_v)^2. \quad (5.3)$$

The values of the required parameters for materials of interest are listed in Table IV. We write

$$\Gamma^{\text{def}} = \sigma^{\text{def}} T, \quad (5.4)$$

and give the values of σ^{def} , obtained from Eq. (5.3), in Table IV.

For materials which lack inversion symmetry, piezoelectric interaction of electrons and holes with acoustic phonons (both LA and TA) must be taken into account. This interaction is known to provide an important scattering mechanism in semiconductors with wurtzite and zinc-blende structures.²⁷⁻²⁹ We rewrite Eq. (2.8) in terms of the piezoelectric constants,³⁰ which are listed in Table V: For cubic structure systems,

$$u_{\mathbf{q}} = (2ee_{14}/\epsilon_0 q^2) [\hbar/2\rho\omega_\sigma(q)]^2 (q_x q_y \xi_z^\sigma + q_y q_z \xi_x^\sigma + q_x q_z \xi_y^\sigma), \quad (5.5)$$

and for wurtzite structure systems,

$$u_{\mathbf{q}} = [e/q^2 \epsilon(\mathbf{q})] [\hbar/2\rho\omega_\sigma(q)] [e_{15}(q_x^2 + q_y^2)\xi_z^\sigma + e_{33}q_z^2\xi_z^\sigma + (e_{15} + e_{31})q_z(q_x \xi_x^\sigma + q_y \xi_y^\sigma)], \quad (5.6)$$

where

$$\epsilon(q) = \epsilon_{11}\sin^2\theta + \epsilon_{33}\cos^2\theta, \quad (5.7)$$

θ is the azimuthal angle,²⁹ and ξ is the polarization unit vector of the phonon.

After summing over polarizations and using a space-averaged ϵ_0 in place of (5.7), we obtain, for the contribution to the linewidth due to the piezoelectric interaction, the following: For cubic structure systems,

$$\Gamma^{\text{piez}}/k_B T = (e^2/14/70\pi)(e^2/\rho\epsilon_0^2\hbar)(3/v_{\text{LA}}^3 + 8/v_{\text{TA}}^3)A^2, \quad (5.8)$$

and for wurtzite structure systems,

$$\Gamma^{\text{piez}}/k_B T = (1/120\pi)(e^2/\rho\epsilon_0^2\hbar)\{(1/v_{\text{LA}}^3)[\frac{4}{3}(e_{31} + 3e_{33}/4 + 2e_{15})^2 + 7e_{33}^2/4] + (2/v_{\text{TA}}^3)[(e_{31} - e_{33} - e_{15}/3)^2 + 56e_{15}^2/9]\}A^2, \quad (5.9)$$

where

$$A = (1 + a_B^* P_e^2)^{-1} - (1 + a_B^* P_h^2)^{-1}. \quad (5.10)$$

We find that the contribution to the linewidth due to the piezoelectric interaction is negligible compared to that from the deformation-potential interaction. The small magnitude of the contribution from the piezoelectric interaction arises from the fact that the electron and hole contributions to A in Eq. (5.10) nearly cancel. A similar situation arises in calculations for resonant Brillouin scattering, where the same factor A makes the ratio of TA- to LA-phonon-scattering efficiencies small.²³ The authors of Ref. 23 suggested that the cancellation in (5.10) is due primarily to the effective-mass approximation, and that a better calculation of the exciton envelope wave function could increase the factor A in (5.8) and (5.9) by up to 1 order of magnitude. Even if this were the case, however, we would find that the contribution of the piezoelectric interaction to the linewidth would be far smaller than from the deformation-potential interaction.

We now consider the effects on the linewidth due to the fact that the initial state of the system is a polariton rather than an exciton. The initial state of the polariton is given by a specified frequency ω , which is taken to correspond to the maximum of the absorption curve. Then the wave vector for the dispersion $k(\omega)$ is obtained by setting the denominator of Eq. (1.2) equal to zero and solving for k . For exciton interactions with acoustic phonons, both phonon absorption and emission can contribute to the linewidth. Because the sound velocity is small, the exciton-acoustic-phonon collision is almost elastic, and after angular integration in k space, one obtains,³¹

$$\Gamma^{\text{def}}/k_B T \simeq (Mk/\pi\rho\hbar^2v^2)(D_e - D_h)^2. \quad (5.11)$$

The resonance condition is defined by $|W - E| < O(E_{\text{LT}})$, so that $k > k_r$, which is defined in Eq. (4.8). If the polariton dispersion $k(\omega)$ is sufficiently flat in the resonance region, then Γ^{def} given in Eq. (5.11) for the polari-

TABLE IV. $D_e - D_h$ are the experimental values for the difference between the deformation-potential coupling constants for electrons and holes, v_{LA} are measured velocities of the LA phonons, and ρ is the mass density. σ^{def} is defined in Eq. (5.4) and gives the contribution to the linewidth parameter from interaction with acoustic phonons. $\sigma_1^{\text{pol}}, \sigma_2^{\text{pol}}$ are defined in Eq. (5.12) and give the contribution to the linewidth parameter including the effects of the resonant interaction between light and excitons, and are evaluated at ω_T and ω_L , respectively. Γ_c is the critical value of the damping parameter obtained from Eq. (5.13).

	$D_e - D_h$ (eV)	v_{LAG} (10^5 cm/s)	ρ (g/cm ³)	σ^{def} (10^{-3} meV/K)	σ_1^{pol} (10^{-3} meV/K)	σ_2^{pol} (10^{-3} meV/K)	Γ_c (meV)
CdTe	-4.5 ^a	3.2	6.20 ^f	0.72	1.46	3.53	0.3
ZnTe	-5.88 ^c	4.0	5.51 ^f	0.55	1.38	2.41	0.92
ZnSe	-6.7 ^d	4.2	5.65 ^f	1.96	3.1	6.90	1.0
GaAs	-9.77 ^b	4.8	5.3 ^c	0.64	0.95	1.12	0.24
InP	-6.35 ^c	4.6	4.78 ^f	0.40	0.64	0.86	0.29
CdS	2.2 ^h	4.2	4.82	0.18	0.35	0.83	1.3
CdSe	-2.17 ⁱ	3.7	5.81	0.06			0.60

^aD. G. Thomas, J. Appl. Phys. Suppl. **32**, 2298 (1961).

^bJ. D. Wiley, Solid State Commun. **8**, 1865 (1970); B. Weber, M. Cardona, C. K. Kim, and S. Rodriguez, Phys. Rev. B **12**, 5729 (1975).

^cH. Müller, R. Trommer, and M. Cardona, Phys. Rev. B **21**, 4879 (1980).

^dM. Cardona and N. E. Christensen, Phys. Rev. B **35**, 6182 (1987).

^eM. Neuberger, *III-V Semiconductor Compounds*, Vol. II of *The Handbook of Electronic Materials* (Plenum, New York, 1971).

^fA. J. Moses, *The Practicing Scientist Handbook* (Van Nostrand/Reinhold, New York, 1978).

^gObtained from the elastic constants given in footnote f above.

^hJ. E. Rowe, M. Cardona, and F. H. Pollak, in *II-VI Semiconducting Compounds*, edited by D. G. Thomas (Benjamin, New York, 1967), p. 112.

ⁱM. Grynberg, in *Proceedings of the 7th International Conference on the Physics of Semiconductors*, edited by M. Hulin (Dunod, Paris, 1965).

ton can be substantially larger than that for the exciton, which is given by Eq. (5.3). In fact, the ratio between them is equal to $k\hbar/Mv$.

Here we treat the lifetimes using a two-branch polariton model²³ in which the dispersion $k(\omega)$ is obtained from Eq. (4.7). The polariton dispersion relations for ZnTe and GaAs are shown in Figs. 2(a) and 2(b), respectively. We now note that scattering from the 1S exciton-polariton state to polariton states formed from the excited states of the exciton can take place. The density of final states for such transitions is very small, and we include only intraband scattering.

It has been argued³² that the maximum in the absorption curve is shifted from the transverse exciton frequency ω_T toward the longitudinal exciton frequency $\omega_L = \omega_T + E_{LT}/\hbar$. Thus we have evaluated the linewidth at both ω_T and ω_L , and we define

$$\Gamma^{ac}(\omega_T) = \sigma_1^{pol} T, \quad \Gamma^{ac}(\omega_L) = \sigma_2^{pol} T. \quad (5.12)$$

The results obtained here for σ_1^{pol} and σ_2^{pol} are given in Table IV for a number of materials. There it is seen that σ_1^{pol} and σ_2^{pol} are considerably greater than σ^{def} , and thus in the case of acoustic-phonon interactions it is important to include the effects of the resonant interaction between the light and the exciton which forms the polariton in treating the linewidth correctly.

The polariton dispersion used here was obtained neglecting the effect of damping on the dispersion relation itself. It is known^{14,24} that this effect can be neglected as long as the total damping, e.g., that in Eq. (1.3), is smaller than the critical value²³ Γ_c , which is given by

$$\Gamma_c/E_{LT} = (8E_T^2\epsilon_0/E_{LT}Mc^2)^{1/2}. \quad (5.13)$$

Values of Γ_c also are given in Table IV. In many of those systems for which experimental data are available,⁴⁻⁶ the magnitudes of the low-temperature damping is comparable to Γ_c , and at higher temperatures the magnitudes can be larger than Γ_c . Thus, a more complete treatment of the polariton dispersion would include a self-consistent treatment of the polariton damping in determining their polariton dispersion. We believe that such a treatment would not substantially affect our results, and we have not carried it out here. We might note that when a two-branch polariton model is not adequate, such as might be the case for the coupled valence bands of zinc-blende systems, a more complicated model, such as a three-branch model,³³ could be used, or the experimental polariton dispersion³⁴ could be used.

We now consider the available experimental data for the linewidths due to acoustic-phonon interactions. The experimental results are obtained by fitting a form like Eq. (1.3) to data for the temperature dependence of the linewidths. The acoustic-phonon contribution dominates the temperature-dependent part of the linewidth only for temperatures $\lesssim 100$ K. The resulting estimates of the parameter σ for the acoustic-phonon contribution from experiment are fairly crude. Segall¹⁰ has noted that the estimate $\sigma \sim 8.6 \times 10^{-3}$ meV/K is consistent with the

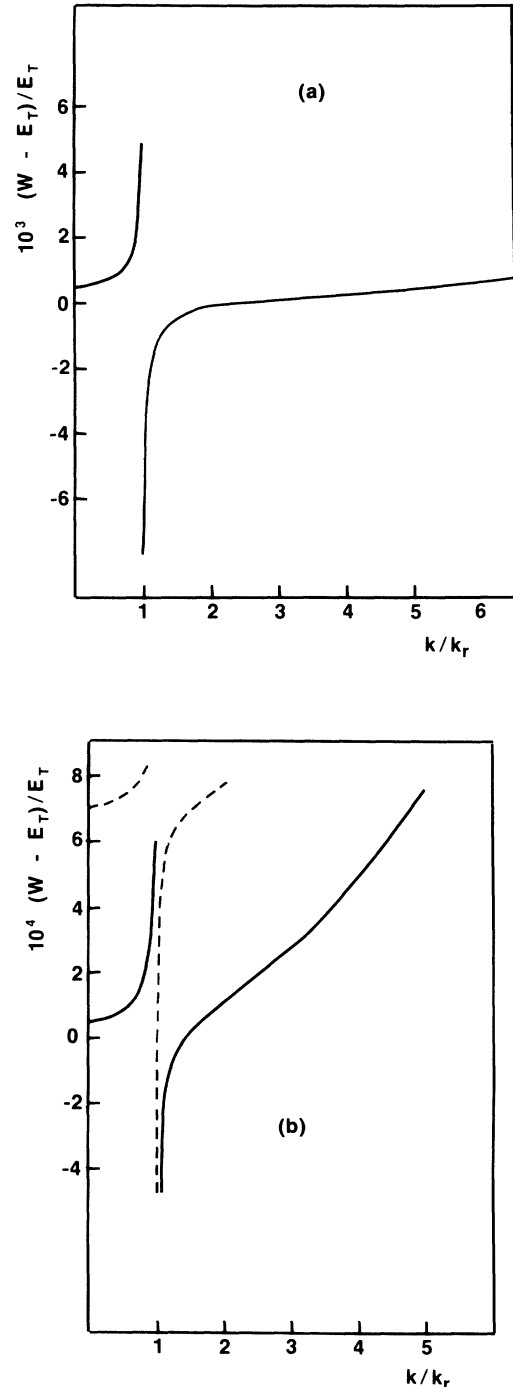


FIG. 2. Polariton dispersions $W(k)$ for two materials based on the two-band model. Here, E_T is the transverse exciton energy measured from the top of the valence band, and k_r , which is defined in Eq. (4.8), is the wave vector for which the exciton and light dispersions cross. The solid curves are the lower and upper polariton branches formed from the 1S exciton, and the dashed curves are for polaritons formed from the first-excited exciton states. (a) The case of ZnSe, for which the parameters are $E_T = 2.80$ eV, $E_{LT} = 1.45$ meV, $\epsilon_0 = 8.8$, and $M = 1.44$, (b) The case of GaAs, for which the parameters are $E_T = 1.515$ eV, $E_{LT} = 0.08$ meV, $\epsilon_0 = 12.35$, and $M = 0.587$.

TABLE V. Values of the components of the piezoelectric tensor taken from experiment. Values in this table are taken from G. Arlt and P. Quadflieg [Phys. Status Solidi **25**, 323 (1968)] and from D. Berlincourt, H. Jaffe, and L. R. Shinozawa, Phys. Rev. **129**, 1009 (1963).

	e_{14} (C/m ²)		
CdTe	0.031		
ZnTe	0.0284		
ZnSe	0.049		
GaAs	0.16		
	e_{15} (C/m ²)	e_{33} (C/m ²)	$e_{33} - e_{31}$ (C/m ²)
CdS	-0.210	0.44	0.731
CdSe	-0.138	0.35	0.507

temperature-dependent linewidth data of Marple⁴ for ZnSe, CdTe, ZnSe, and ZnTe, and that the same value is also consistent with the data of Gutsche and Voigt⁵ on CdS. We have fitted the data for the temperature dependence of the linewidth of the Alperovich *et al.*⁶ for GaAs and obtain the estimate $\sigma \sim 12 \times 10^{-3}$ meV/K. Schultheis *et al.*³⁵ have given an estimate of $\sigma \sim 8 \times 10^{-3}$ meV/K for GaAs based on optical-dephasing experiments. We are not in a position to estimate the uncertainties in these experimental values. The theoretical results in Table IV are less than these experimental values. We do not currently understand the origin of this discrepancy. Some additional theoretical consideration may be necessary.

$$(d_{1S,1S}^{LO})^2 = C_1 \left[\frac{5}{32} (h_e + h_h) - \frac{1}{2} h_e h_h (h_e^3 + h_h^3) / (h_e^2 - h_h^2)^2 + 2 (h_e h_h)^3 / (h_e^2 - h_h^2) (h_e + h_h) \right]. \quad (6.3)$$

Here, $h_i = M/m_i$, and

$$C_1 = 4R_0 \hbar \omega_{LO} (\mu / \epsilon_0 m_0) (\epsilon_\infty^{-1} - \epsilon_0^{-1}). \quad (6.4)$$

For the systems in Table I, we find that $\Gamma/D < 0.3$ up to room temperature. Thus the line shape should be Lorentzian, and the treatment given here for the linewidth, based on perturbation theory for the exciton-phonon interaction, is appropriate. For temperatures large compared to $\hbar\omega$, the ratio goes as $T^{1/2}$, so, in principle, at high enough temperatures, the line might become Gaussian.

For the interaction with acoustic phonons, we obtain, from the deformation-potential interaction,

$$D_{1S}^{ac} = [4\hbar / (\pi^2 a_B^* \rho v)] \int_0^\infty dx x^3 \{ 1 + 2[\exp(2\hbar v x / a_B^* k_B T) - 1]^{-1} \} [D_e / (1 + x^2 h_e^{-2}) - D_v / (1 + x^2 h_h^{-2})]. \quad (6.5)$$

For this interaction, we obtain Γ/D in the range 0.1–0.3 up to room temperature, and thus this contribution to the line shape is also Lorentzian.

VII. SUMMARY

We have presented a detailed treatment of the exciton linewidth due to the interaction of the exciton with LO phonons and with acoustic phonons. Complete summa-

VI. “WEAK COUPLING” VERSUS “STRONG COUPLING” IN THE EXCITON-PHONON INTERACTION

The theory of the absorption line shape given by Eq. (1.1) is obtained by retaining only second-order terms in the exciton self-energy.^{1,2,25} This approximation is appropriate for weak exciton-phonon interaction or for a wide exciton band. If one considers the case of strong interaction or of a sufficiently narrow band, then, to the lowest approximation, the exciton dispersion can be neglected. Then, for energies away from the resonance, one can resum^{25,36} the perturbation series for the exciton Green’s function to obtain a Gaussian line shape for the absorption, with the half-width D given by^{25,36}

$$D_{1S}^2 = V \sum_\lambda \int d^3q (2\pi)^{-3} (2N_q + 1) |V_{\lambda,1S}|^2. \quad (6.1)$$

Here the exciton-phonon interaction matrix element $V_{\lambda,1S}$ is given by Eq. (2.5), and N_q is a phonon occupation number.

Toyozawa^{1,36} derived a criterion to distinguish this “strong-coupling” case from the “weak-coupling” case in which lowest-order perturbation theory is appropriate. He compared a correlation time given by $\tau_c = \hbar\Gamma/D^2$, with a relaxation time given by $L(\tau_R) = 1$, where $L(\tau)$ is the Fourier transform of the linewidth. He found that the linewidth is Lorentzian if $\Gamma/D \ll 1$, and that it is Gaussian if $\Gamma/D \gg 1$, where Γ is given by Eq. (2.10).

Here we estimate D_{1S} , the value of D for the 1S state, by the intraband contribution $D_{1S,1S}$, and we compare it to the intraband contribution to the linewidth, $\Gamma_{1S,1S}$. The result for LO-phonon coupling is

$$D_{1S,1S}^{LO} = (2N_{LO} + 1)^{1/2} d_{1S,1S}^{LO}, \quad (6.2)$$

where

tions over all intermediate states of the exciton, including the exact scattering states of the continuum, have been included. The effects of the resonant interaction between photons and excitons to form polaritons have been taken into account. Results for LO-phonon coupling for a series of compound semiconductors are in generally good agreement with available experimental data. Results for acoustic-phonon coupling are smaller than current experimental estimates.

ACKNOWLEDGMENTS

This work was supported in part by the U.S. Office of Naval Research (ONR) (T.L.R.). This work was done

while one of us (S.R.) was at the Naval Research Laboratory with financial support from the National Research Council (NRC).

APPENDIX

In this Appendix we give two lengthy expressions which occur in the evaluation of the LO-phonon contribution to the exciton linewidth. The quantities $\Delta_n(q_1)$ that occur in the contribution of the discrete states in Eq. (3.14) are

$$\begin{aligned} \Delta_n(q_1) = & (2/n)^4 \{ n [t_e^3 r_e^{2(n-2)} (A_e'^2 + A_e''^2) + t_h^3 r_h^{2(n-2)} (A_h'^2 + A_h''^2)] \\ & + \frac{1}{6} n(n-1)(2n-1) (t_e^3 r_e^{2(n-2)} B_e^2 + t_h^3 r_h^{2(n-2)} B_h^2) + n(n-1) (t_e^3 r_e^{2(n-2)} B_e A_e'' + t_h^3 r_h^{2(n-2)} B_h A_h'') \\ & - (t_e t_h)^{3/2} (r_e r_h)^n {}^{-2} [2a_1 D_1' + (D_2' a_2 + D_2'' a_3) + \frac{1}{2} B_e B_h a_4] \} \end{aligned} \quad (\text{A1})$$

where q_1 is defined by Eq. (3.3), and the other parameters in this expression are given by

$$r_i^2 = \frac{(1-1/n)^2 + a_B^{*2} Q_i^2}{(1+1/n)^2 + a_B^{*2} Q_i^2}, \quad (\text{A2})$$

$$t_i^2 = [(1+1/n)^2 + a_B^{*2} Q_i^2]^{-1}, \quad (\text{A3})$$

$$A_i = r_i \exp(i\beta_i) + nr \exp(-i\beta_i) - (n-1) \exp(-i\gamma_i), \quad (\text{A4})$$

$$B_i = 2r_i (\sin\beta_i - \sin\gamma_i), \quad (\text{A5})$$

$$A_i' = \text{Re } A_i, \quad A_i'' = \text{Im } A_i, \quad (\text{A6})$$

$$a_1 = \sin(un) / \sin u, \quad (\text{A7})$$

$$a_2 = (n-1)a_1, \quad (\text{A8})$$

$$a_3 = [a_1 - n \cos(un) / \cos u] \cot u, \quad (\text{A9})$$

$$a_4 = [n^2 - (n-1)^2] a_1 + 2n \cos(un) \cot u / \sin u - \sin(un) \cot^2 u / \sin u - \sin(un) / \sin^3 u, \quad (\text{A10})$$

$$u = \alpha_e - \alpha_h, \quad (\text{A11})$$

$$\tan\alpha_i = (2a_B^* Q_i / n) (1 - 1/n^2 + a_B^{*2} Q_i^2)^{-1}, \quad (\text{A12})$$

$$\tan\beta_i = Q_i a_B^* / (1 + 1/n), \quad \gamma_i = \alpha_i + \beta_i, \quad (\text{A13})$$

$$D_1' = A_e' A_h' + A_e'' A_h'', \quad (\text{A14})$$

$$D_1'' = A_e'' A_h' - A_e' A_h'', \quad (\text{A15})$$

$$D_2' = A_h'' B_e + A_e'' B_h, \quad (\text{A16})$$

$$D_2'' = A_h' B_e - A_e' B_h. \quad (\text{A17})$$

The quantities F_{ee} , F_{hh} , and F_{eh} that occur in Eq. (3.23) for the contribution from the continuum states in the case of LO-phonon interactions are given by

$$F_{ee} = (r_{1e} r_{2e})^{-6} (m_e / m_h)^2 y [(m_e / m_h)^2 y^2 + (1+x^2)/3], \quad (\text{A18})$$

$$F_{hh} = (r_{1h} r_{2h})^{-6} (m_h / m_e)^2 y [(m_h / m_e)^2 y^2 + (1+x^2)/3], \quad (\text{A19})$$

$$\begin{aligned} F_{eh} = & (r_{1e} r_{2e} r_{1h} r_{2h})^{-3} y x [\sin(d/x) / \sinh(d)] \\ & \times \cos(2\delta_1 + d/x) \exp(-\delta_2/x) \\ & \times [y^2 + y\tau_1 (m_e / m_h - m_h / m_e) - \tau_1^2 - \tau_2], \end{aligned} \quad (\text{A20})$$

where

$$r_{1i}^2 = 1 + (s_i + x)^2, \quad (\text{A21})$$

$$r_{2i}^2 = 1 + (s_i - x)^2, \quad (\text{A22})$$

$$d = \ln(r_{1e} r_{2h} / r_{2e} r_{1h}), \quad (\text{A23})$$

$$y^2 = x_0^2 - x^2, \quad (\text{A24})$$

$$\delta_{1,2} = \phi_{1e} + \phi_{2e} \pm (\phi_{1h} + \phi_{2h}), \quad (\text{A25})$$

$$\tau_1 = x \coth d - \cot(d/x), \quad (\text{A26})$$

$$\tau_2 = (x / \sinh d)^2 - 1 / \sin^2(d/x), \quad (\text{A27})$$

$$s_e = y m_e / m_h, \quad (\text{A28})$$

$$s_h = -y m_h / m_e, \quad (\text{A29})$$

$$\tan\phi_{1i} = x + s_i, \quad (\text{A30})$$

$$\tan\phi_{2i} = x - s_i, \quad (\text{A31})$$

$$x_0 = (\mu / m_0)^{-1/2} \epsilon_0 (E_0 / R_0)^{1/2}. \quad (\text{A32})$$

*Present address.

- ¹Y. Toyozawa, *Prog. Theor. Phys.* **20**, 53 (1958); *J. Phys. Chem. Solids* **25**, 59 (1964).
- ²B. Segall and G. D. Mahan, *Phys. Rev.* **171**, 935 (1968).
- ³J. J. Hopfield, *Phys. Rev.* **112**, 1555 (1958).
- ⁴D. T. F. Marple (unpublished).
- ⁵E. Gutsche and J. Voigt, in *Proceedings of the International Conference on II-VI Semiconducting Compounds, Providence, RI, 1967*, edited by D. G. Thomas (Benjamin, New York, 1967), p. 337.
- ⁶V. L. Alperovich, V. M. Zaletin, A. F. Kravchenko, and A. S. Terekhov, *Phys. Status Solidi B* **77**, 465 (1976).
- ⁷D. S. Chemla, D. A. B. Miller, P. W. Smith, A. C. Gossard, and W. Wiegmann, *IEEE J. Quantum Electron.* **QE-20**, 265 (1984).
- ⁸O. J. Glembocki, B. V. Shanabrook, and W. T. Beard, *Proceedings of the 2nd International Conference on Modulated Compounds, Kyoto, 1985* [*Surf. Sci.* **174**, 201 (1985)].
- ⁹J. Lee, E. S. Koteles, and M. O. Vassell, *Phys. Rev. B* **33**, 5512 (1986); H. N. Spector, J. Lee, and P. Melman, *ibid.* **34**, 2554 (1986).
- ¹⁰B. Segall, in *Proceedings of the IXth Conference on the Physics of Semiconductors, Moscow, 1968*, edited by S. M. Ryvkin (Nauka, Leningrad, 1968), p. 425.
- ¹¹S. Rudin and T. L. Reinecke, *Phys. Rev. B* **41**, 3017 (1990).
- ¹²B. Segall, *Phys. Rev.* **150**, 734 (1966); **163**, 769 (1967); G. E. Hite, D. T. F. Marple, M. Aven, and B. Segall, *ibid.* **156**, 850 (1967).
- ¹³Y. Osaka, Y. Imai, and Y. Takeuti, *J. Phys. Soc. Jpn.* **24**, 236 (1968).
- ¹⁴W. C. Tait, *Phys. Rev. B* **5**, 648 (1972).
- ¹⁵O. Madelung, *Introduction to Solid State Theory* (Springer-Verlag, Berlin, 1978).
- ¹⁶E. Hanamura and H. Haug, *Phys. Rep.* **33C** 221 (1977).
- ¹⁷C. Kittel, *Quantum Theory of Solids* (Wiley, New York, 1963).
- ¹⁸G. D. Mahan, in *Polarons in Ionic Crystals and Polar Semiconductors*, edited by J. T. Devreese (North-Holland, Amsterdam, 1972), p. 553.
- ¹⁹L. D. Landau and E. M. Lifshitz, *Quantum Mechanics—Nonrelativistic Theory* (Pergamon, London, 1965).
- ²⁰P. M. Morse and H. Feshbach, *Methods of Theoretical Physics* (McGraw-Hill, New York, 1953).
- ²¹H. Fröhlich, in *Polarons and Excitons*, edited by C. G. Kuper and G. D. Whitfield (Plenum, New York, 1963), p. 1.
- ²²G. Beni and T. M. Rice, *Phys. Rev. B* **15**, 840 (1977).
- ²³C. Weisbuch and R. G. Ulbrich, in *Light Scattering in Solids III*, edited by M. Cardona and G. Güntherodt (Springer-Verlag, Berlin, 1982), pp. 207–263.
- ²⁴M. Matsushita, J. Wicksted, and H. Z. Cummins, *Phys. Rev. B* **29**, 3362 (1984).
- ²⁵V. M. Agranovich, *Theory of Excitons* (in Russian) (Nauka, Moscow, 1968).
- ²⁶E. O. Kane, *Phys. Rev. B* **11**, 3850 (1975).
- ²⁷A. R. Hutson and D. L. White, *J. Appl. Phys.* **33**, 40 (1962); G. D. Mahan and J. J. Hopfield, *Phys. Rev. Lett.* **12**, 241 (1964).
- ²⁸D. Berlincourt, H. Jaffe, and L. R. Shiozawa, *Phys. Rev.* **129**, 1009 (1963).
- ²⁹G. Arlt and P. Quadflieg, *Phys. Status Solidi* **25**, 323 (1968); G. Arlt, *J. Appl. Phys.* **36**, 2317 (1965).
- ³⁰The components of the piezoelectric coupling tensor as defined in Ref. 18 [from which Eqs. (5.5) and (5.6) are obtained] differ by factor 4π from the definitions usually quoted in the literature (e.g., Refs. 28 and 29); thus the numerical factor in our equations is different from those in Ref. 18.
- ³¹W. C. Tait and R. L. Weiher, *Phys. Rev.* **166**, 769 (1968).
- ³²W. C. Tait and R. L. Weiher, *Phys. Rev.* **178**, 1404 (1969); additional discussion on the effective absorption curve can be found in V. V. Travnikov and V. V. Krivolapchuk, *Zh. Eksp. Teor. Fiz.* **85**, 2087 (1983) [*Sov. Phys.—JETP* **58**, 1210 (1983)].
- ³³G. Fishman, *Solid State Commun.* **27**, 1097 (1978).
- ³⁴Some of the experimental work on polariton dispersions is reviewed in Ref. 23.
- ³⁵L. Schultheis, A. Honold, J. Kuhl, K. Koehler, and C. W. Tu, in *Proceedings of the 18th International Conference on the Physics of Semiconductors, Stockholm, 1986*, edited by O. Engström (World Scientific, Singapore, 1987), p. 1397.
- ³⁶S. Nakajima, Y. Toyozawa, and R. Abe, *The Physics of Elementary Excitations* (Springer-Verlag, Berlin, 1980).